Saturn Impact Trajectories for Cassini End-of-Life

Chit Hong Yam
Diane Craig Davis
James M. Longuski
Kathleen C. Howell

School of Aeronautics and Astronautics
Purdue University
West Lafayette, Indiana 47907

2007 AAS/AIAA Astrodynamics Specialists Conference

Saturn Impact Trajectories for Cassini End-of-Life

Chit Hong Yam,[*] Diane Craig Davis,[†] James M. Longuski[‡] and Kathleen C. Howell[§]

School of Aeronautics and Astronautics, Purdue University, West Lafayette, Indiana 47907-2045

We design Saturn impact trajectories for the end-of-life of the Cassini spacecraft. For short-period orbits (6-10 days), we use a Tisserand graph to determine when the ring-plane crossing distance is within the ring-gap to reencounter Titan. To impact Saturn with short-period orbits, the spacecraft hops through the rings of Saturn via successive Titan flybys to place the periapsis in Saturn's atmosphere. For long-period orbits (550-900 days), solar gravity plus a small apoapse maneuver can lower the spacecraft's periapsis to impact Saturn. For certain orbits with periods > 900 days, no maneuver is necessary, providing an attractive "flyby-and-forget" option.

I.   Introduction

After extraordinary success in exploring the Saturnian system,[1] including an extended mission,[2] the final options for the Cassini spacecraft must be ultimately decided. We consider the potential for an "encore mission" and a controlled end-of-life mission for Cassini. As in the case of the Galileo mission,[3] one option may be to plunge the Cassini spacecraft into the atmosphere of Saturn, ensuring the spacecraft's destruction and avoiding collision with any of the satellites (and other undesired events) so that future scientific investigations will not be contaminated or compromised.

Titan, being the largest moon of Saturn, is the only satellite in the Saturnian system that can serve as an effective gravity-assist body. Since its arrival at Saturn in July 2004, Cassini has performed over 30 flybys at Titan (and up to 45 Titan flybys have been planned through July 2008).[4–7] For tour design, we use Titan-to-Titan resonance transfers to pump the energy up (or down) and to crank the inclination (as described in Refs. 6–8) to achieve the desired conditions.

One of the science objectives of the Cassini/Huygens mission is to observe the structure and dynamic behavior of Saturn's rings.[9] However, Saturn's rings pose a hazard, as debris from the rings can damage the spacecraft. Passage through the ring plane is considered safe as long as the node crossing occurs either within a gap in the rings or beyond the G ring (i.e., $r > 2.92$ R$_S$). For example, upon arrival at Saturn in July 2004, Cassini passed through the gap between the G ring and the F ring.[4–6]

We consider two options for Saturn impact in this paper. For short-period orbits (6-10 days), we use Titan's gravity-assist to drop the periapsis down to Saturn's atmosphere; for long-period orbits (>550 days), we employ solar perturbations to reduce the periapsis radius to achieve an impact. Other works examine alternative end-of-life scenarios, such as placing Cassini into a stable orbit about Saturn with periapsis just above Titan's orbit[10] or a long-term trajectory

---

[*] Doctoral Candidate, Student Member AAS, Student Member AIAA; email: cyam@purdue.edu.
[†] Ph.D. Student, Student Member AIAA; email: decraig@purdue.edu.
[‡] Professor, Member AAS, Associate Fellow AIAA; email: longuski@purdue.edu.
[§] Hsu Lo Professor of Aeronautical and Astronautical Engineering, Fellow AAS, Associate Fellow AIAA; email: howell@purdue.edu.

beyond the orbit of Phoebe,[11] or using gravity assists from Titan to eject Cassini from the Saturnian system to impact Jupiter, Uranus, or Neptune.[12]

II.   Cassini-Huygens Mission (Background)

After the encounters at Saturn by Pioneer 11 and Voyagers 1 and 2, plans for a Saturn orbiter began in 1982 that later became the Cassini-Huygens mission.[13,14] References 15–17 describe the primary science objectives, which include observations of: the rings, the magnetosphere, Titan, and other satellites. Some important discoveries from the mission are reported in Refs. 18 and 19 on finding water vapor plumes on Enceladus, confirming the presence of lakes of liquid methane on Titan,[20] and in Refs. 21 and 22 announcing the detection of new moons.

After 7 years of interplanetary cruise,[23] the Cassini orbiter was inserted into orbit about Saturn in July 2004,[1] while the Huygens probe was delivered through the atmosphere of Titan in January 2005.[24,25] References 26–28 describe the engineering operations and maneuver experience during the mission. The Cassini primary mission is scheduled through July 2008 with the possibility of an extended mission lasting until June 2010.[2,29]

III.   Analysis

In this section we review the technique of gravity assist. We present expressions for relationships between the orbital elements about the central body, which aid the design of gravity-assist impact trajectories. Effects of solar gravity are included.

Touring in the Saturnian System
For short-period impact trajectories, we employ a two-body, patched-conic model.[30,31] Such a model assumes that the spacecraft is in a two-body conic orbit about the central body (e.g., Saturn). A gravity-assist flyby of a satellite (e.g., Titan) is regarded as an instantaneous change in velocity relative to the central body. Period (and size) of the spacecraft orbit can be increased (or decreased) via orbit pumping,[32] while orbit cranking changes the inclination of the spacecraft orbit relative to the central body.[8]

To reach a desired final condition (e.g., Saturn impact), we use a series of Titan-to-Titan transfers (i.e., a tour) to control the orbital parameters. Successive Titan flybys can be assured when the spacecraft enters a resonance orbit: the ratio of the spacecraft's period and the satellite's period is a rational number (i.e., fraction of integers). Let n be the number of gravity-assist body (Titan) orbits about the central body and m be the number of spacecraft orbits (before the next Titan encounter) about the central body. For an $n{:}m$ resonance orbit (where m and n are integers), the period of the spacecraft T_{sc} can be found as

$$T_{sc} = \left(n/m \right) T_{ga} \tag{1}$$

where T_{ga} is the period of the gravity-assist body, Titan. The semi-major axis a_{sc} and the period of the spacecraft T_{sc} are related by

$$a_{sc} = \left[\mu_{cb} \left(T_{sc}/2\pi \right)^2 \right]^{1/3} \tag{2}$$

where μ_{cb} is the gravitational parameter of the central body, Saturn.

V_∞ in terms of Orbital Parameters

At the moment of encountering the gravity-assist (GA) body, the position (from the central body) of the spacecraft and the position of the gravity-assist body are equal, i.e.,

$$\mathbf{r}_{sc} = \mathbf{r}_{ga} \tag{3}$$

$$r_{enc} = \|\mathbf{r}_{sc}\| = \|\mathbf{r}_{ga}\| \tag{4}$$

where r_{enc} is the encounter distance from the central body and $\mathbf{r}_{sc}$ and $\mathbf{r}_{ga}$ are the position vectors of the spacecraft and the GA body (Titan), respectively and bold denotes a vector. The hyperbolic excess velocity, or V_∞, is the velocity vector of the spacecraft relative to the GA body before or after an encounter. The excess velocity vector, V_∞, is the difference between the velocity of the spacecraft, V_{sc}, and the velocity of the GA body, V_{ga}, i.e.,

$$\mathbf{V}_\infty = \mathbf{V}_{sc} - \mathbf{V}_{ga} \tag{5}$$

Following an approach similar to Strange and Sims,[33] we can write V_{sc} and V_{ga} in a coordinate frame tied to the orbit plane of the GA body, $\hat{\mathbf{p}}_1 - \hat{\mathbf{p}}_2 - \hat{\mathbf{p}}_3$, as

$$\mathbf{V}_{sc} = v_{sc} \left(\sin\gamma_{sc}\hat{\mathbf{p}}_1 + \cos\gamma_{sc}\cos i_{rel}\hat{\mathbf{p}}_2 + \cos\gamma_{sc}\sin i_{rel}\hat{\mathbf{p}}_3 \right) \tag{6}$$

$$\mathbf{V}_{ga} = v_{ga} \left(\sin\gamma_{ga}\hat{\mathbf{p}}_1 + \cos\gamma_{ga}\hat{\mathbf{p}}_2 \right) \tag{7}$$

$$\hat{\mathbf{p}}_1 = \mathbf{r}_{ga}/\|\mathbf{r}_{ga}\| \qquad \hat{\mathbf{p}}_3 = \mathbf{r}_{ga} \times \mathbf{V}_{ga}/\|\mathbf{r}_{ga} \times \mathbf{V}_{ga}\| \qquad \hat{\mathbf{p}}_2 = \hat{\mathbf{p}}_3 \times \hat{\mathbf{p}}_1 \tag{8}$$

where γ_{sc} and γ_{ga} are the flight path angles of the spacecraft and the GA body, respectively. Instead of using Saturn's equator, we use the gravity-assist body's (i.e., Titan's) orbit plane as the reference plane (similar to the approach of Strange[34]). We note that the angle i_{rel} in Eq. (6) is the inclination of the spacecraft orbit relative to the GA body's orbit plane (i.e., the angle between the angular momentum vectors of the spacecraft orbit and the GA body's orbit), where i_{rel} ranges from $-180°$ to $180°$. Positive i_{rel} indicates that the encounter is at the ascending node (relative to the GA body's orbit), i.e., the spacecraft is approaching from below the reference plane; and negative i_{rel} indicates that the encounter is at the descending node, i.e., the spacecraft is approaching from above the GA's orbit plane. Substituting Eqs. (6) and (7) into Eq. (5) gives

$$\mathbf{V}_\infty = \left(v_{sc}\sin\gamma_{sc} - v_{ga}\sin\gamma_{ga} \right)\hat{\mathbf{p}}_1 + \left(v_{sc}\cos\gamma_{sc}\cos i_{rel} - v_{ga}\cos\gamma_{ga} \right)\hat{\mathbf{p}}_2 + \left(v_{sc}\cos\gamma_{sc}\sin i_{rel} \right)\hat{\mathbf{p}}_3 \tag{9}$$

A dot product of V_∞ with itself in Eq. (9) yields an expression of the magnitude (as provided in Refs. 33 and 34):

$$\mathbf{V}_\infty \cdot \mathbf{V}_\infty = v_\infty^{\,2} = v_{sc}^{\,2} + v_{ga}^{\,2} - 2v_{sc}v_{ga}\left(\sin\gamma_{sc}\sin\gamma_{ga} + \cos\gamma_{sc}\cos\gamma_{ga}\cos i_{rel} \right) \tag{10}$$

Since a gravity assist can change the direction, but not the magnitude of the $\mathbf{V}_\infty$, Eq. (10) provides a relationship between the spacecraft orbital parameters: v_{sc}, γ_{sc}, and i_{rel} for a given set of GA orbital parameters: v_{ga} and γ_{ga}. For Titan-to-Titan resonance transfers, in theory, the spacecraft encounters Titan at the same inertial location (i.e., r_{ga} and $\mathbf{V_{ga}}$ do not change) and the v-infinity magnitude ($v_\infty = \|\mathbf{V}_\infty\|$) remains constant. In practice, perturbations (e.g., solar and J_2) may shift the Titan reencounter location. The velocity (relative to the central body) and the flight path angle can be written as

$$v^2 = \mu\left(2/r - 1/a\right) \tag{11}$$

$$\cos\gamma = \frac{h}{rv} = \frac{\sqrt{\mu a\left(1-e^2\right)}}{rv} = \frac{\sqrt{\mu p}}{rv} \tag{12}$$

$$\sin\gamma = \pm\sqrt{1-\cos^2\left(\gamma\right)} = \pm\frac{\sqrt{r^2 v^2 - \mu p}}{rv} \tag{13}$$

where $p = a(1 - e^2)$ is the semi-latus rectum. The $\pm$ sign in Eq. (13) corresponds to outbound orbits (+) and inbound orbits (−) respectively. We can rewrite Eq. (10) in terms of the semi-major axis and the semi-latus rectum by substitution of Eqs. (11)–(13):

$$
\begin{aligned}
4 - v_\infty^2\big/\left(\mu_{cb}/r_{enc}\right) &= r_{enc}/a_{sc} + r_{enc}/a_{ga} + 2\Big[\left(\sqrt{p_{sc}/r_{enc}}\right)\left(\sqrt{p_{ga}/r_{enc}}\right)\cos i_{rel} \\
&\quad \pm\left(\sqrt{2 - r_{enc}/a_{sc} - p_{sc}/r_{enc}}\right)\left(\sqrt{2 - r_{enc}/a_{ga} - p_{ga}/r_{enc}}\right)\Big]
\end{aligned}
\tag{14}
$$

where a_{sc} and a_{ga} are the semi-major axes of the spacecraft orbit and the GA body, p_{sc} and p_{ga} are the semi-latus rectums of the spacecraft orbit and the GA body. The $\pm$ sign in Eq. (14) corresponds to the combinations of outbound/inbound orbits of the spacecraft and the GA body: positive (+) when both spacecraft and GA body are outbound or when both are inbound (i.e., product of the flight path angles $\gamma_{sc}\gamma_{ga} > 0$); negative (−) when one is outbound and one is inbound (i.e., product of the flight path angles $\gamma_{sc}\gamma_{ga} < 0$). We note that Eq. (14) is the Tisserand criterion[35–37] for elliptic GA body orbit. For a circular GA body orbit, $a_{ga} = p_{ga} = r_{enc}$ yields (as given by Strange and Longuski[37])

$$3 - v_\infty^2\big/\left(\mu_{cb}/r_{enc}\right) = r_{enc}/a_{sc} + 2\cos i_{rel}\sqrt{p_{sc}/r_{enc}} \tag{15}$$

Equation (14) [or (15)] provides an invariant relationship between the semi-major axis, a_{sc}, the semi-latus rectum, p_{sc}, and the inclination, i_{rel} for gravity-assist trajectories. In designing the Europa orbiter mission, Heaton et al.[38] assumes circular orbits for the GA bodies (Galilean satellites) and coplanar orbits for the GA bodies and the spacecraft. For designing Saturn impact trajectories, however, we cannot neglect the eccentricity of Titan (as we will see later) and therefore Eq. (14) is used instead of Eq. (15).

V_∞ in terms of Pump and Crank Angles

Equation (9) offers a way to express the V_∞ in terms of the velocity, the flight path angle, and the inclination (v_{sc}, γ_{sc}, and i_{rel}). We introduce another way to parameterize the V_∞ in terms of the pump angle α and the crank angle κ as

$$\mathbf{V}_\infty = v_\infty \left(\sin\alpha \cos\kappa \hat{\mathbf{q}}_1 + \cos\alpha \hat{\mathbf{q}}_2 - \sin\alpha \sin\kappa \hat{\mathbf{q}}_3 \right) \tag{16}$$

where the unit vectors $\hat{\mathbf{q}}_1 - \hat{\mathbf{q}}_2 - \hat{\mathbf{q}}_3$ are given by

$$\hat{\mathbf{q}}_2 = \mathbf{V}_{ga} / \left\| \mathbf{V}_{ga} \right\| \qquad \hat{\mathbf{q}}_3 = \mathbf{r}_{ga} \times \mathbf{V}_{ga} / \left\| \mathbf{r}_{ga} \times \mathbf{V}_{ga} \right\| \qquad \hat{\mathbf{q}}_1 = \hat{\mathbf{q}}_2 \times \hat{\mathbf{q}}_3 \tag{17}$$

The pump angle α is the angle between the v-infinity vector and the velocity of the GA body with respect to the central body (see Figure 1). The magnitude of the spacecraft velocity can be found by applying the cosine law on the $\mathbf{V}_{ga}$-$\mathbf{V}_\infty$-$\mathbf{V}_{sc}$ triangle:

$$v_{sc}^2 = v_{ga}^2 + v_\infty^2 - 2v_\infty v_{ga} \cos\alpha \tag{18}$$

The pump angle α can range from 0° to 180°. It is directly related to the spacecraft speed v_{sc} (and hence the orbital energy and semi-major axis) relative to the central body. Less energetic orbits have bigger pump angles and vice versa. For given v_{ga} and v_∞, $\alpha = 0^o$ and $\alpha = 180^o$ represents the most energetic and the least energetic orbits possible (respectively) for encountering the GA body.

The crank angle κ is an angle measured in the plane perpendicular to the GA body's orbit plane (see Figure 1), where the reference line for zero-κ is $\hat{\mathbf{q}}_1$ (where $\hat{\mathbf{q}}_1 = \hat{r}_{ga}$ when GA body's orbit is circular). (In Figure 1, we have illustrated a case where $\kappa > 180^o$ for aesthetic reasons.) The crank angle κ can range from -180° to 180°. It measures how "inclined" the V_∞ is relative to the GA body's orbit plane. When $\kappa = 0^o$ or 180°, the $\mathbf{V}_{ga}$-$\mathbf{V}_\infty$-$\mathbf{V}_{sc}$ triangle lies on the GA body's orbit plane, which means the spacecraft and the GA body share the same orbit plane (i.e., $i_{rel} = 0^o$ or 180°). The quadrant of κ can also provide information of the encounter type at the GA body: $0^o < \kappa < 180^o$ means the encounter is descending (i.e., spacecraft approaching the GA body from above the reference plane); $-180^o < \kappa < 0^o$ means the encounter is ascending; $-90^o < \kappa < 90^o$ means encounter is outbound (i.e., spacecraft is approaching its apoapsis); $90^o < \kappa < 180^o$ or $-180^o < \kappa < -90^o$ means inbound encounter (i.e., spacecraft is approaching its periapsis).

Equations (9) and (16) are expressions of the V_∞ in terms of two sets of parameters (α, κ and v_{sc}, γ_{sc}, i_{rel}) and we are interested in the relationship between them. The unit vectors $\hat{\mathbf{q}}_1 - \hat{\mathbf{q}}_2 - \hat{\mathbf{q}}_3$ can be written in terms of $\hat{\mathbf{p}}_1 - \hat{\mathbf{p}}_2 - \hat{\mathbf{p}}_3$ as

$$\hat{\mathbf{q}}_1 = \cos\gamma_{ga} \hat{\mathbf{p}}_1 - \sin\gamma_{ga} \hat{\mathbf{p}}_2 \qquad \hat{\mathbf{q}}_2 = \sin\gamma_{ga} \hat{\mathbf{p}}_1 + \cos\gamma_{ga} \hat{\mathbf{p}}_2 \qquad \hat{\mathbf{q}}_3 = \hat{\mathbf{p}}_3 \tag{19}$$

Substituting Eq. (19) into Eq. (16) and comparing coefficients of $\hat{\mathbf{p}}_1$, $\hat{\mathbf{p}}_2$ and $\hat{\mathbf{p}}_3$ with Eq. (9) yields

$$v_{sc} \sin \gamma_{sc} \qquad = v_\infty \left(\cos\alpha \sin\gamma_{ga} + \sin\alpha \cos\kappa \cos\gamma_{ga} \right) + v_{ga} \sin\gamma_{ga} \tag{20}$$

$$v_{sc} \cos\gamma_{sc} \cos i_{rel} = v_\infty \left(\cos\alpha \cos\gamma_{ga} - \sin\alpha \cos\kappa \sin\gamma_{ga} \right) + v_{ga} \cos\gamma_{ga} \tag{21}$$

$$v_{sc} \cos\gamma_{sc} \sin i_{rel} = -v_\infty \sin\alpha \sin\kappa \tag{22}$$

For a given v-infinity magnitude (v_∞) and given GA body's parameters (v_{ga} and γ_{ga}), we can use Eqs. (18), and (20)–(22) to solve for spacecraft orbital parameters (v_{sc}, γ_{sc}, and i_{rel}) from pump and crank angles (α and κ), and vice versa (we can solve for pump and crank angles from spacecraft orbital parameters).
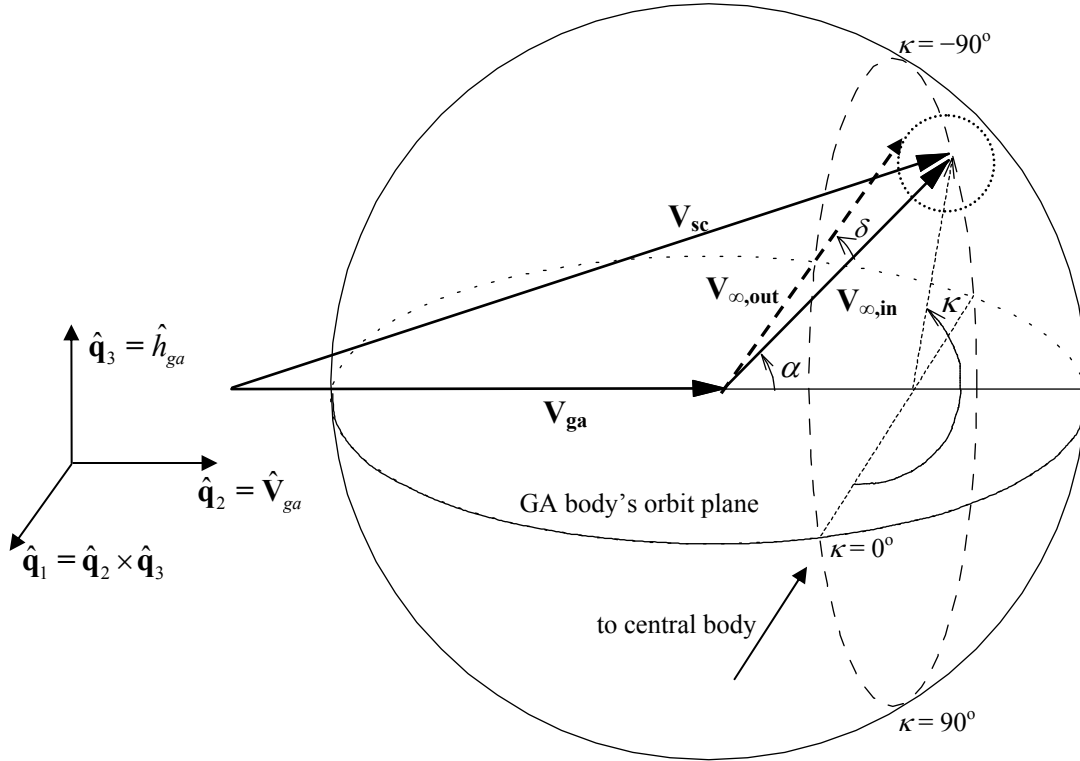

Figure 1: The V_∞ sphere (after Strange[39] and Rinderle[40]).
The illustration shows $\kappa > 180^o$ for aesthetic reasons.

Bending of V_∞ after Flyby

A gravity-assist flyby rotates V_∞ while keeping the magnitude (v_∞) constant. That is, a satellite (e.g., Titan) encounter *bends* the incoming (pre-flyby) v-infinity vector ($\mathbf{V_{\infty,in}}$) into the outgoing (post-flyby) v-infinity vector ($\mathbf{V_{\infty,out}}$). The angle between $\mathbf{V_{\infty,in}}$ and $\mathbf{V_{\infty,out}}$ is referred to as the bending angle δ, given by

$$\sin\left(\delta/2\right) = 1 \Big/ \left[1 + \left(h_p + R_{ga} \right) v_\infty^2 \Big/ \mu_{ga} \right] \tag{23}$$

where h_p is the flyby altitude, R_{ga} is the radius of the gravity-assist body, and μ_{ga} is the gravitational parameter of the gravity-assist body, Titan. From Eq. (23), we note that the

bending angle only depends on the flyby altitude h_p (since other quantities are constant during flyby). A lower flyby altitude produces a larger bending of the $\mathbf{V}_\infty$ (and hence a bigger change in orbital elements about the central body). For a given incoming v-infinity vector ($\mathbf{V}_{\infty,\text{in}}$) and flyby altitude h_p (or bending angle δ), the outgoing v-infinity vector ($\mathbf{V}_{\infty,\text{out}}$) is given as

$$\mathbf{V}_{\infty,\text{out}} = v_\infty \left(-\sin\delta\cos\theta \; \hat{\mathbf{b}}_1 - \sin\delta\sin\theta \; \hat{\mathbf{b}}_2 + \cos\delta \; \hat{\mathbf{b}}_3 \right) \tag{24}$$

$$\hat{\mathbf{b}}_3 = \mathbf{V}_{\infty,\text{in}} / \left\| \mathbf{V}_{\infty,\text{in}} \right\| \qquad \hat{\mathbf{b}}_1 = \hat{\mathbf{b}}_3 \times \hat{\mathbf{n}} / \left\| \hat{\mathbf{b}}_3 \times \hat{\mathbf{n}} \right\| \qquad \hat{\mathbf{b}}_2 = \hat{\mathbf{b}}_3 \times \hat{\mathbf{b}}_1 \tag{25}$$

where θ is the flyby B-plane angle (where $-180°<\theta\leq180°$), $\hat{\mathbf{n}}$ is the unit pole vector $= 0\hat{x}+0\hat{y}+\hat{z}$, where $\hat{x}-\hat{y}-\hat{z}$ are the Cartesian unit vectors of the reference frame (e.g., Saturn equator and equinox of epoch).

Figure 1 illustrates a $\mathbf{V}_\infty$ sphere with radius equal to the magnitude of the v-infinity (v_∞). The pump and crank angles can be defined (as described previously) for any $\mathbf{V}_\infty$, incoming or outgoing. [The pump and crank angles (α and κ) in Figure 1 refers to $\mathbf{V}_{\infty,\text{in}}$.] A constant bending angle δ with a sampling of the B-plane angle θ from $-180°$ to $180°$ creates a small circular locus on the v-infinity sphere for the outgoing v-infinity vector ($\mathbf{V}_{\infty,\text{out}}$). Each point on the $\mathbf{V}_{\infty,\text{out}}$-circle represents a different post-flyby orbit about the central body and a different set of post-flyby pump and crank angles. Once we determine the pump and crank angles for $\mathbf{V}_{\infty,\text{out}}$ [from Eqs. (16) and (24)], orbital elements after the flyby can be solved through Eqs. (18), (20)–(22). Also, the area inside the $\mathbf{V}_{\infty,\text{out}}$-circle corresponds to flybys with a bending angle smaller than δ (or flyby higher than an altitude of h_p). Thus, the $\mathbf{V}_{\infty,\text{out}}$-circle provides a way to predict the family of outgoing orbits after a single flyby with a constraint on the flyby altitude (e.g., $h_p \geq 1000$ km at Titan).

Vacant Node Crossing Distance and Rings

The ascending and descending nodes are the locations where the orbit intersects with the reference plane. In our patched-conic analysis, we use the GA body's orbit plane (Titan's orbit) as the reference plane, which constrains the GA body's encounter to be at one of the nodes. (We note that Titan's orbit is slightly inclined ($0.365°$) relative to Saturn's equator, the ring plane.) Figure 2 shows a typical Cassini orbit about Saturn, where the Titan encounter is at the descending node (i.e., the spacecraft approaches Titan from above the reference plane). Besides the Titan encounter, the spacecraft also intersects with the reference plane at the ascending node while the GA body is not present. Such a node crossing is referred to as a vacant node.[34] We define the distance from Saturn's center to the vacant node as r_{vac}. The vacant node crossing distance, r_{vac}, can be written in terms of the semi-latus rectum, p_{sc}, and the encounter distance, r_{enc}, as

$$r_{vac} = \frac{1}{2/p_{sc} - 1/r_{enc}} \tag{26}$$

(See Strange[34] for derivation.) To avoid damage to the spacecraft, the node crossing should occur either within a gap between the F and G rings or beyond the G ring; i.e., the node crossing must satisfy the following criteria

$$2.347 \; R_S < r_{vac} < 2.730 \; R_S \qquad \text{or} \qquad r_{vac} > 2.917 \; R_S \tag{27}$$

(For descriptions of Saturn's ring system, see Cuzzi et al.[17]) We assume the spacecraft can safely pass through the ring plane as long as its node crossing satisfies Eq. (27).

For Titan-to-Titan resonance transfers, the encounter distance r_{enc} is constant (in theory) and r_{vac} only depends on the semi-latus rectum, p_{sc}. We can find expressions relating p_{sc} and the pump and crank angles by summing the squares of Eqs. (21) and (22):

$$\left(v_{sc}\cos\gamma_{sc}\sin i_{rel}\right)^2 + \left(v_{sc}\cos\gamma_{sc}\cos i_{rel}\right)^2 = \left(v_{sc}\cos\gamma_{sc}\right)^2 = \left(h_{sc}/r_{enc}\right)^2 = \mu_{cb}p_{sc}/\left(r_{enc}^2\right)$$

$$\Rightarrow \mu_{cb}p_{sc}/\left(r_{enc}^2\right) = \left[v_\infty\left(\cos\alpha\cos\gamma_{ga} - \sin\alpha\cos\kappa\sin\gamma_{ga}\right) + v_{ga}\cos\gamma_{ga}\right]^2 + \left(v_\infty\sin\alpha\sin\kappa\right)^2$$

(28)

Once we know the encounter distance and the v-infinity magnitude (and the other GA body's parameters), Equations (26) and (28) can be used to find orbits satisfying the constraint on the ring plane crossing distance [Eq. (27)].
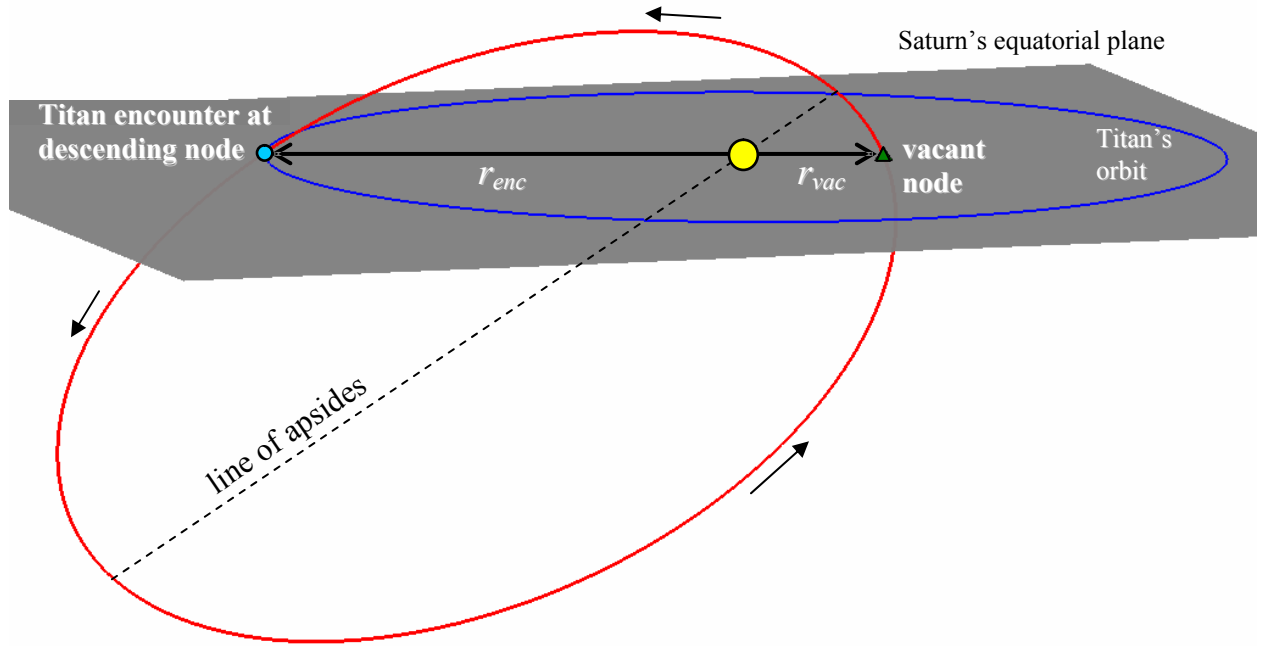

Figure 2: Titan encounter and the vacant node.

Effects of Solar Gravity by Quadrant

The impact of the Sun as a perturbing force can be significant on large orbits about Saturn (a distance of 9 to 10 AU from the Sun). The direction of the perturbing acceleration that originates with solar gravity depends on the orientation of the spacecraft's orbit relative to the Sun and Saturn (see Patterson et al.[10] and Davis et al.[11]). Thus, to investigate this force and exploit it for trajectory design, observation from the perspective of a coordinate frame that rotates with Saturn about the Sun is insightful. A Saturn-centered rotating frame is defined to facilitate the analysis. Let the $\hat{x} - \hat{y}$ plane represent Saturn's orbital plane. The $\hat{x} - $axis is fixed along the Sun-Saturn line, and the $\hat{y} - $axis is perpendicular to the $\hat{x} - $axis in Saturn's orbital plane. The $\hat{y} - $axis is defined as positive in the direction of Saturn's motion. Four quadrants, centered at Saturn, are

defined in the rotating frame and appear in Figure 3. The quadrants are defined in a counterclockwise fashion, with quadrant I on the far side of Saturn and leading Saturn in its orbit. When the spacecraft orbit is viewed in this rotating frame, its orientation is defined by the quadrant that contains the orbit apoapsis. In the current work, the angle of orientation, ϕ, within each quadrant is defined as the angle from the Sun-Saturn line. The positive sense of the angle in each quadrant is defined in Figure 3. (We note that other authors have used different definitions to describe orientation.[41])
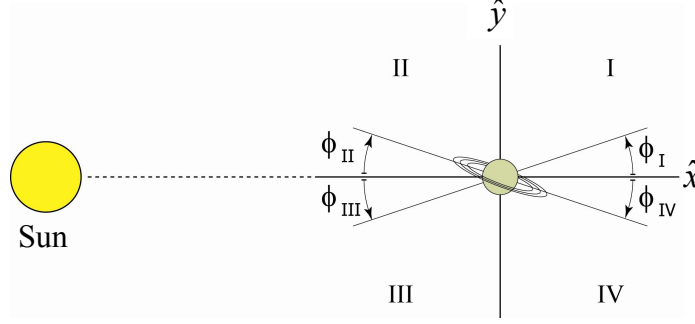

Figure 3: Quadrants and orientation angles as defined in the rotating frame (Davis et al.[11]).

Let us consider a prograde orbit large enough to be perturbed significantly by the Sun but sufficiently small such that the solar gravitational perturbations do not cause the orbit to become retrograde or to escape. If the apoapsis originally lies in quadrants I or III, solar gravity will lower the periapse radius, increase eccentricity, and increase v_∞ with respect to Titan at a subsequent encounter. Alternatively, if apoapsis lies in quadrants II or IV, solar gravity will raise the periapse radius, decrease eccentricity, and decrease v_∞ with respect to Titan. These results are summarized in Table 1.

Table 1: Effects of Solar Gravitational Perturbations Relative to the Previous Orbit (Davis et al.[11])

Parameter	Quadrants I and III	Quadrants II and IV
Semi-major axis	decreases	increases
Periapsis radius	decreases	increases
Eccentricity	increases	decreases
v_∞ wrt Titan	increases	decreases

For a given orbit at a specified orientation angle, the solar gravitational perturbations have maximum effect when the orbit lies in the ecliptic plane. We note that Saturn's equatorial plane is inclined at about 26.7° with respect to the ecliptic. Also, within each quadrant, solar perturbations are at a maximum when the apoapsis lies at approximately 45° from the Sun-Saturn line (see Figure 3), although the precise value varies as the period of the orbit changes. For large orbits, the orientation of the Sun-Saturn line with respect to the spacecraft orbit line of apsides shifts while the spacecraft is in transit about Saturn, due to Saturn's motion about the Sun, affecting the value of the optimal orientation. The changes in semi-major axis, periapse radius, and eccentricity from one revolution to the next as functions of angle ϕ_I in quadrant I for a 957-

day orbit appear in Figure 4. Of course, once $\phi_I > 90°$, the orbit has shifted into another quadrant. Thus, the quantities increase and decrease consistent with the quadrant.
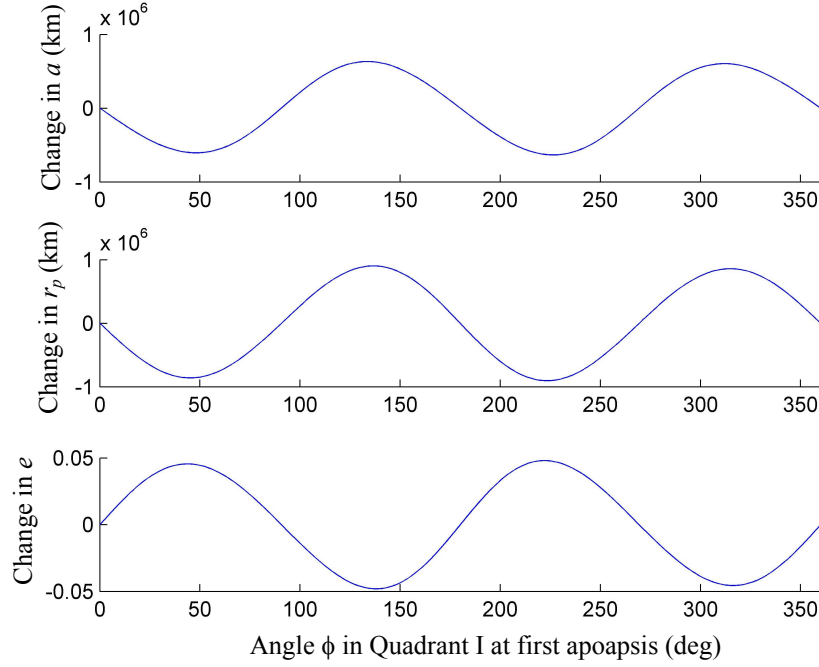

Figure 4: Changes in orbital elements from one revolution to the next as a function of quadrant angle ϕ_I: 957-day orbit (Davis et al.[11]).

The solar effects on an orbit obviously increase as the apoapse radius increases. Thus, for long-period orbits, the effects of solar gravity can be significant. For an orbit of sufficiently large period, with apoapsis in quadrant I or quadrant III, solar gravity can lower periapse radius such that impact with the planet occurs.

IV.   Numerical Results

Assumptions and Constraints

The Cassini primary mission is scheduled through July 2008 with the possibility of an extended mission lasting until June 2010.[2,29] Table 2 summarizes two sets of initial conditions for the end-of-life scenarios, one that originates from the end of the primary mission and one that originates from the end of the proposed extended mission. We assume that a trajectory ends in impact when the periapse radius, r_p, is less than one Saturnian radius, 1 R_S. Perturbations from J_2 and higher order harmonics (of Saturn) are not included in our analysis (for both short-period and long-period orbits).

The end-of-life options are subjected to the following general constraints: 1) ΔV budget of 50 m/s; 2) minimum flyby altitude at Titan of 1000 km (the last Titan flyby is allowed to be 900 km); 3) the spacecraft should not cross the rings of Saturn [see Eq. (27)] to avoid damaging the spacecraft (except when it is on its way to impact Saturn); and 4) the time for clean-up maneuver after the last Titan flyby should be minimized.

Table 2: Initial Conditions for Cassini End-of-Life Scenario

Parameter	Values
Initial Condition A (ICA): End of Primary Mission	
Titan Encounter Time	July 31, 2008, 03:19:55
v_∞ with respect to Titan	5.887 km/s
Titan's distance from Saturn	19.70 R_S
Orbital Period	7.09 days
Periapse Radius	2.97 R_S
Inclination (wrt Saturn's equator)	75°
Apoapse Orientation (wrt the Sun)	$\phi_{II} = 21.7^o$
Initial Condition B (ICB): End of Extended Mission[a]	
Titan Encounter Time	June 21, 2010, 01:28:22
v_∞ with respect to Titan	5.490 km/s
Titan's distance from Saturn	20.21 R_S
Orbital Period	15.9 days
Periapse Radius	2.64 R_S
Inclination (wrt Saturn's equator)	1.7^o
Apoapse Orientation (wrt the Sun)	$\phi_{IV} = 89.4^o$

[a] As of this writing, the Cassini Extended Mission is proposed, but not officially approved. In this paper, we use a representative Cassini state for the end of the proposed extended mission.

Table 3: Constants for Patched-Conic Analysis

Parameter	Values[a]
Gravitational Parameter of Saturn ($\mu_{Saturn} = \mu_{cb}$)	37931269.2 km^3/s^2
Radius of Saturn (R_S)	60268 km
Gravitational Parameter of Titan ($\mu_{Titan} = \mu_{ga}$)	8978.2 km^3/s^2
Radius of Titan (R_T)	2575 km
Orbital Period of Titan ($T_{Titan} = T_{ga}$)	15.945 days
Semi-major axis of Titan's orbit ($a_{Titan} = a_{ga}$)	1221215 km (= 20.263 R_S)
Eccentricity of Titan's orbit ($e_{Titan} = e_{ga}$)	0.0288
Inclination[b] of Titan's orbit ($i_{Titan} = i_{ga}$)	0.365^o

[a] Constants extracted from JPL's de405 and sat125 ephemeris.
[b] Inclination relative to Saturn's equator.

Models for Trajectory Design and Trajectory Propagation

Patched-Conic Propagation

We use a patched-conic propagator called STOUR to calculate short-period impact trajectories. The satellite tour design program (STOUR) is a software tool developed by JPL for the Galileo mission design.[40] The program has been enhanced and extended at Purdue University to perform automated design of gravity-assist tours of the Solar System and of the satellite system of Jupiter.[42-45] STOUR uses the patched-conic method to calculate gravity-assist trajectories meeting specified requirements. Table 3 shows the parameters of Saturn and Titan used (by STOUR) in the short-period impact analysis.

Model for Long-Period Orbits

Numerical analysis for long-period orbits is accomplished using MATLAB and its ode45 integrator. Tolerances (absolute and relative) are fixed at 1×10^{-12}. Initial conditions and gravitational parameters (GM) values for the Sun and Saturn are extracted from the JPL de408 ephemeris and for Titan from the sat424l ephemeris. Their positions are then integrated along with the spacecraft state. All integrations are performed in the Earth equator and equinox of J2000 inertial frame. The integration software was verified by the full ephemeris, multi-body package Generator-C, developed at Purdue.[46] The initial epoch for the spacecraft is 15-JUN-2009 (i.e., JD = 2454997.54725) for each orbit investigated. Initial conditions for the spacecraft are provided by STOUR and are initiated at a Titan flyby. The constants and assumptions used in this analysis are listed in Table 4.

Table 4: Constants and Assumptions for Numerical Integrations

Parameter	Values
μ_{Saturn}	$3.794062606113728\times10^{7}$ [km^3/s^2]
μ_{Sun}	$1.327124400179870\times10^{11}$ [km^3/s^2]
μ_{Titan}	$8.978137176189042\times10^{3}$ [km^3/s^2]
JD of ICs	2454997.54725
Reference frame	Earth equator and equinox of J2000
Integrator	Matlab ode45
Tolerances (relative and absolute)	1.00E-12
ICs for Saturn, Titan	de408

Summary of Impact Trajectories

We present two Saturn impact options for Cassini end-of-life: a short-period option and a long-period option. For the short-period impact, the spacecraft lower its periapsis by successive Titan-to-Titan resonance transfers. The spacecraft enters the ring gap with a period of 6 to 10 days and an inclination of 50° to 70° and reencounters Titan to reduce the periapsis below Saturn's atmosphere. Depending on Titan's location at encounter (i.e., the radial distance from Saturn), a list of resonance orbits (e.g., 1:2, 3:5, 4:9) are possible to achieve an impact and also to satisfy the constraint on the node distance (as presented in Table 5). We note that the maneuver costs for short-period trajectories are zero in the patched-conic model. In a higher fidelity model that includes the J_2 perturbation, however, a non-zero maneuver cost is expected: the J_2 perturbation can rotate the line of apsides and thus a maneuver may be required to maintain the spacecraft's node within the ring gap. We also expect some maneuver costs associated with station keeping in high inclination orbits.

For long-period orbits, with periods of 550 to 950 days, Saturn impact can be achieved using solar perturbations together with an apoapse ΔV (from 0 to 100 m/s) to lower the periapsis into Saturn's atmosphere. The orientation of the spacecraft orbit must stay around 45° in quadrants I and III (see Figure 3) relative to the Sun-Saturn line and the inclination can range from 0° to 40°. The desired orientation can be reached via a series of outbound-inbound (or inbound-outbound) transfers (see Wolf and Smith[7] for detailed descriptions). Excluding the time of the phasing orbits, assuming the spacecraft is in a 16-day orbit, the total time required (before the ultimate Titan flyby) is ~140 days (for final period of 550 days) to 220 days (for a final period of 950 days) which requires 3 to 4 Titan flybys. For periods > 950 days, the solar perturbation alone

can be sufficient (i.e., no apoapse maneuver is necessary) to reduce the periapsis down to below 1 R_S, providing an attractive "flyby-and-forget" option (i.e., the spacecraft will impact Saturn without any control once the final Titan flyby is performed correctly) for Cassini end-of-life scenario.

Option 1: Saturn Impact via Short-Period Orbit

To find short-period impact orbits, we first characterize orbits at Saturn with a constant v_∞ relative to Titan. According to the Tisserand criterion in Eq. (14), for any given two of a_{sc}, p_{sc}, and i_{rel} (the semi-major axis, the semi-latus rectum, and the inclination relative to Titan's orbit), we can solve for the remaining orbital parameter. The semi-major axis, a_{sc}, is related to the orbital period, T_{sc}, from Eq. (2) and the semi-latus rectum, p_{sc}, is related to the vacant node distance, r_{vac}, from Eq. (26).
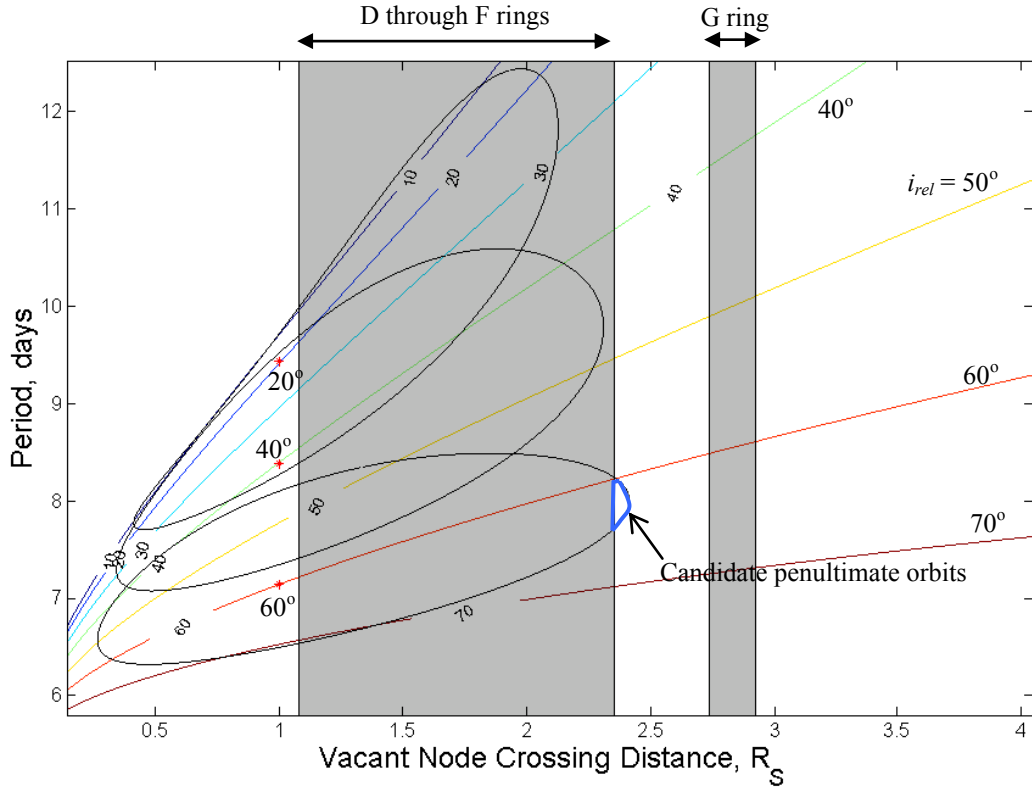

Figure 5: Node crossing distances for various periods and inclinations (relative to Titan's orbit) [v_∞ = 5.490 km/s, h_p = 900 km, r_{enc} = 20.21 R_S, $\gamma_{sc}\gamma_{ga}$ > 0]. Impact orbits (r_{vac} = 1 R_S) with i_{rel} = 20°, 40°, 60° are indicated in red asterisks and ovals represent families of penultimate orbits. The ovals are projections of the small $V_{\infty,out}$-circle (determined by the maximum bending angle, δ) illustrated in Figure 1.

Figure 5 shows a sampling of the T_{sc}-r_{vac}-i_{rel} solution space for a v_∞ of 5.490 km/s (taken from *ICB* of Table 2), where the third dimension of i_{rel} is indicated by contour lines. The shaded areas (in grey) are regions of the rings through which the spacecraft is not allowed to pass [i.e., the constraint on the node distance given by Eq. (27)]. Impact trajectories with a vacant node distance of one Saturnian radius are indicated in red asterisks. (We use r_{vac} = 1 R_S instead of r_p = 1 R_S to simplify our calculations here.) In terms of the sequence of Titan-to-Titan transfers,

13

impact orbits correspond to the ultimate (i.e., final) Titan flyby. To find penultimate (i.e., second-to-last) orbits, we consider a reverse of the ultimate Titan flyby: the incoming excess velocity vector, $V_{\infty,in}$, is derived from an impact orbit (i.e., a red asterisk) and we determine the family of the outgoing orbits by setting the flyby altitude to its minimum (i.e., 900 km) with a sampling of the B-plane angle from -180° to 180°. The three ovals in Figure 5 are families of penultimate orbits which impact Saturn with inclinations of 20°, 40°, and 60°. The ovals demarcate the boundaries where orbits inside the ovals flyby at altitudes higher than 900 km (i.e., satisfy the altitude constraint at Titan). We note that these ovals are essentially the $V_{\infty,out}$-circles (see Figure 1) mapped over the T_{sc}-r_{vac}-i_{rel} solution space.

Among the three ovals of penultimate orbits in Figure 5, only one of them (the impact with an inclination of 60°) extends to the gap between the F and G rings (i.e., a feasible region). The highlighted region in Figure 5 contains the set of periods (T_{sc}) and inclinations (i_{rel}) required for feasible penultimate orbits (which can impact Saturn after a single Titan flyby). We collect all these "pockets" of candidate penultimate orbits in Figure 6 (indicated by the blue curve). Also plotted in Figure 6 are penultimate orbits with different encounter conditions at Titan (i.e., the radial distance of Titan from Saturn at encounter, r_{enc}, and the sign of the product of the flight path angles, $\gamma_{sc}\gamma_{ga}$). We note that the range of periods and inclinations of penultimate orbits widens as the encounter distance, r_{enc}, increases. An intuitive explanation is that the encounter distance, r_{enc}, acts as a leveraging arm of an apoapse ΔV to reduce the periapsis of the spacecraft orbit (where a Titan flyby can be thought as an equivalent velocity change relative to Saturn); the longer the encounter distance, the more effective the ΔV in reducing the periapsis (< 1 R_S).
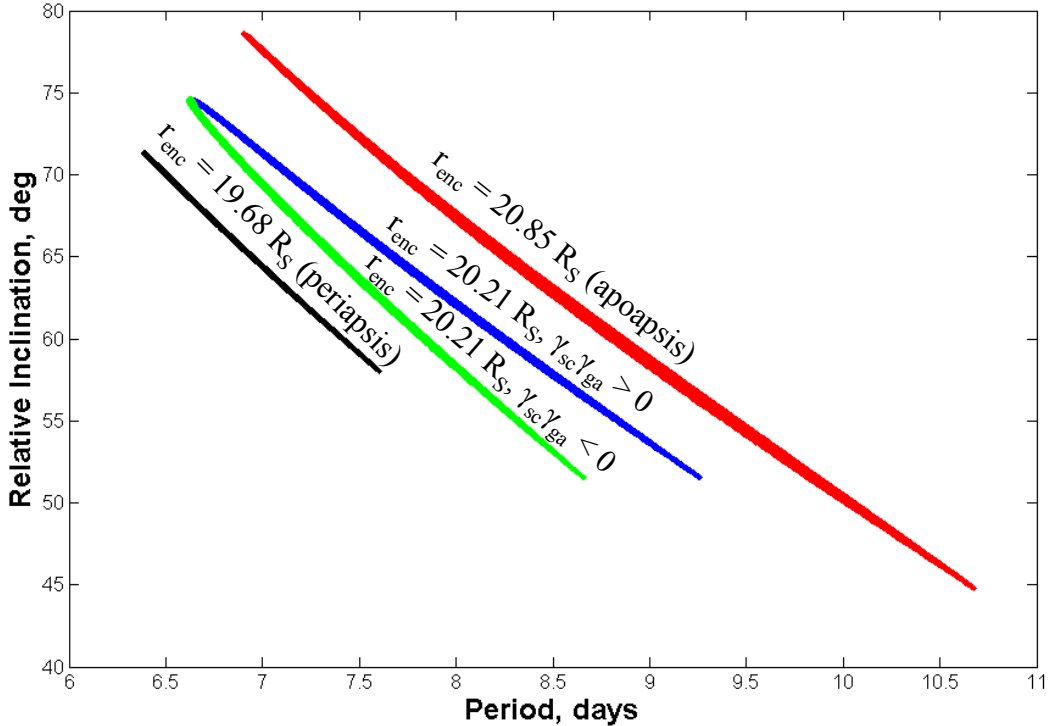

Figure 6: **Penultimate impact orbits with node crossing inside the ring gap [v_∞ = 5.490 km/s, h_p = 900 km]. Points of the blue curve are collection of "candidate penultimate orbits" in Figure 5.**
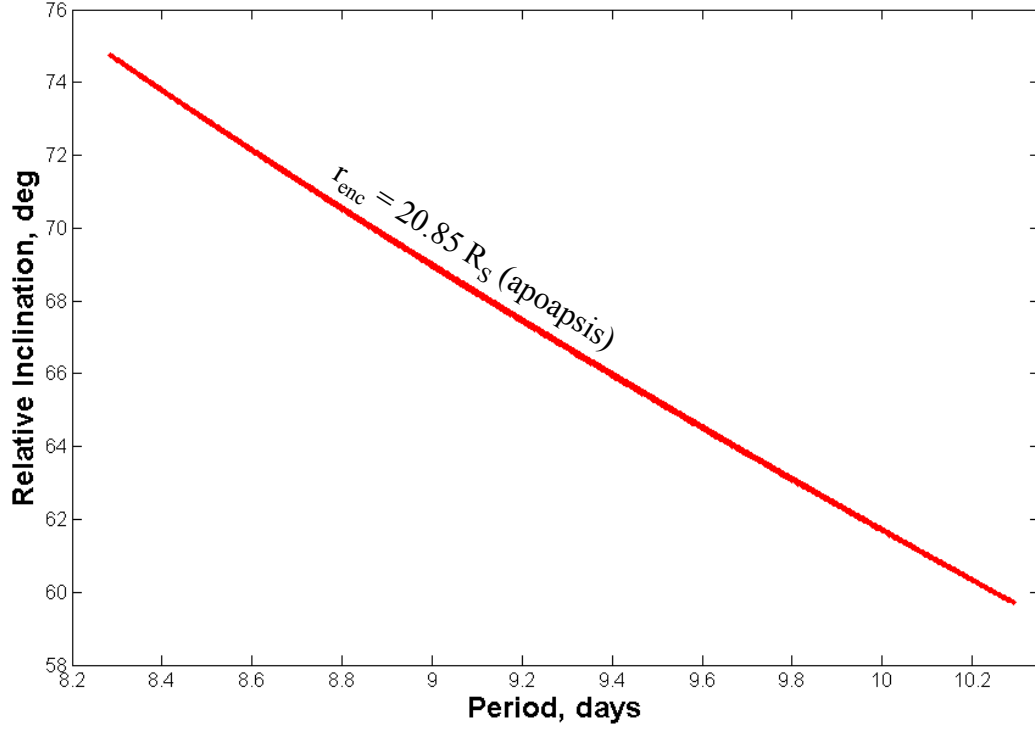
Figure 7: Penultimate impact orbits with node crossing inside the ring gap [v_∞ = 5.889 km/s, h_p = 900 km].

Figure 7 shows the periods and inclinations of penultimate orbits for a v_∞ of 5.889 km/s (taken from *ICA* of Table 2). No orbit was found for an encounter distance less than 20.66 R_S (which is why only one curve of r_{enc} = 20.85 R_S is plotted in Figure 7). We note a higher v_∞ value is more restrictive in the encounter distance since the bending angle in a single Titan flyby is smaller [see Eq. (23)].

Some orbits from Figure 6 and Figure 7 are selected (based on whether the period makes a rational fraction with Titan's orbital period) and we summarize their characteristic in Table 5. The pump and crank angles provided in Table 5 are for the convenience of using a patched-conic propagator like STOUR. (STOUR asks the user to input the resonance ratio and the change in crank angle for each event.) Table 5 provides a range of selection of impact trajectories (for different Titan encounter conditions), which can impact Saturn in 4 to 9 months (112 days to 287 days) using 5 to 10 Titan flybys. Periods of the penultimate orbits range from 6 to 10 days with inclinations of ~50° to 70°. To achieve an impact from a 16-day equatorial orbit, we should first crank up the inclination to 40° to 50° (in 1:1 resonance orbits), then pump down the period (and crank up the inclination together) using 3:4 and 3:5 resonance orbits. The higher the inclination and the lower the period of the penultimate orbits, the more intermediate Titan flybys are required (in general) to achieve an impact.

Table 5: Selected Penultimate Impact Trajectories

Titan: S/C Revs	Period, days	Inclination, deg[a]	Pump Angle, deg	Crank Angle, deg[b]	Number of Titan Flybys[c]	Min. Flyby Altitude, km[d]	Total Time of Flight, days[e]
$v_\infty = 5.490$ km/s		$r_{enc} = 20.21$ R$_S$, $\gamma_{sc}\gamma_{ga} > 0$					
1:2	7.97	62.30	142.0	42.06	7	1000	159
3:7	6.83	72.85	151.1	66.72	10	1000	287
4:7	9.11	52.75	136.0	32.17	6	900	191
4:9	7.09	70.45	148.6	57.52	9	1000	239
$v_\infty = 5.490$ km/s		$r_{enc} = 20.21$ R$_S$, $\gamma_{sc}\gamma_{ga} < 0$					
1:2	7.97	58.45	142.0	40.03	7	1000	159
3:7	6.83	71.40	151.1	65.66	10	1000	287
4:9	7.09	68.30	148.6	56.25	8	1000	223
$v_\infty = 5.490$ km/s		$r_{enc} = 20.85$ R$_S$ (apoapsis)					
1:2	7.97	67.50	144.4	45.86	8	1000	175
2:3	10.63	45.19	132.0	25.47	5	900	112
3:5	9.57	53.60	135.9	31.48	5	1000	128
4:7	9.11	57.30	138.0	34.51	6	1000	223
4:9	7.09	76.55	151.8	68.47	10	1000	255
$v_\infty = 5.490$ km/s		$r_{enc} = 19.68$ R$_S$ (periapsis)					
3:7	6.83	66.20	148.5	56.52	9	900	223
4:9	7.09	63.40	146.3	50.03	8	900	223
5:11	7.25	61.71	145.0	46.97	8	900	239
$v_\infty = 5.889$ km/s		$r_{enc} = 20.85$ R$_S$ (apoapsis)					
3:5	9.57	64.77	137.8	34.52	7	900	159
4:7	9.11	68.13	139.8	37.20	8	900	223

[a] Relative to Titan's orbit plane.
[b] Only the principal values of the crank angle κ are presented. Other quadrants of κ can be calculated from the principal values.
[c] Number of Titan flybys required to impact Saturn from a 16-day equatorial orbit.
[d] Minimum flyby altitude of the final Titan flyby (all non-ultimate flybys have altitudes ≥ 1000 km).
[e] Total flight time from a 16-day equatorial orbit to final Titan flyby (exclude time to impact).

Choice of Sampling Parameter

As a side note, we describe some details of the sampling of orbital parameters for creating Figure 5. For a given i_{rel}, the orbital period T_{sc} of an impact orbit ($r_{vac} = 1$ R$_S$) can be solved from Eqs. (2) and (14). However, we note that orbits with $i_{rel} > \sim 75°$ are not feasible for $v_\infty = 5.490$ km/s. (An expression of maximum inclination can be found in Uphoff et al.[8]) Therefore i_{rel} is not a convenient parameter for sampling. Instead of i_{rel}, we use the crank angle κ to calculate orbits with various inclinations. For a given crank angle, κ, from Eq. (28), we can solve for the corresponding pump angle, α, such that $r_{vac} = 1$ R$_S$. We also note from Eq. (28) that the sign of κ does not change p_{sc} (and hence r_{vac}), which means an ascending Titan encounter (negative κ) and a descending Titan encounter (positive κ) produce the same vacant node distance. The pump and crank angles (α and κ) are related to T_{sc}-r_{vac}- i_{rel} through Eqs. (2), (11)-(13), (18), and (20)-(22). The crank angle κ can range from 0° to 90° for outbound Titan encounters or from 90° to 180° for inbound Titan encounters. Once we know the pump and crank angles corresponding to an impact trajectory, we can determine its $\mathbf{V}_\infty$ relative to Titan from Eq. (16).

Sample Itinerary of Short-Period Impact

As an example, we provide a short-period impact trajectory propagated using STOUR. Table 6 shows the itinerary of an impact trajectory and Figure 8 plots its trajectory. The initial state of this trajectory is taken from *ICB* of Table 2 (i.e., end of the proposed extended mission). We first crank up the inclination of the spacecraft orbit to ~40° in three 1:1 resonance transfers. We then pump down the period (and crank up simultaneously) with a 3:4 and a 3:5 resonance orbit. The spacecraft enters the ring gap (with r_{vac} = 2.360 R$_S$) with a period of 8 days (1:2 resonance), orbits Saturn for two revs and reencounters Titan after 16 days. A final Titan flyby lowers the periapsis to 0.993 R$_S$ (59,865 km) and the spacecraft impacts Saturn's atmosphere in 5 days. The total time to impact (since *ICB*) is 160 days; 7 Titan flybys are required for this scenario.
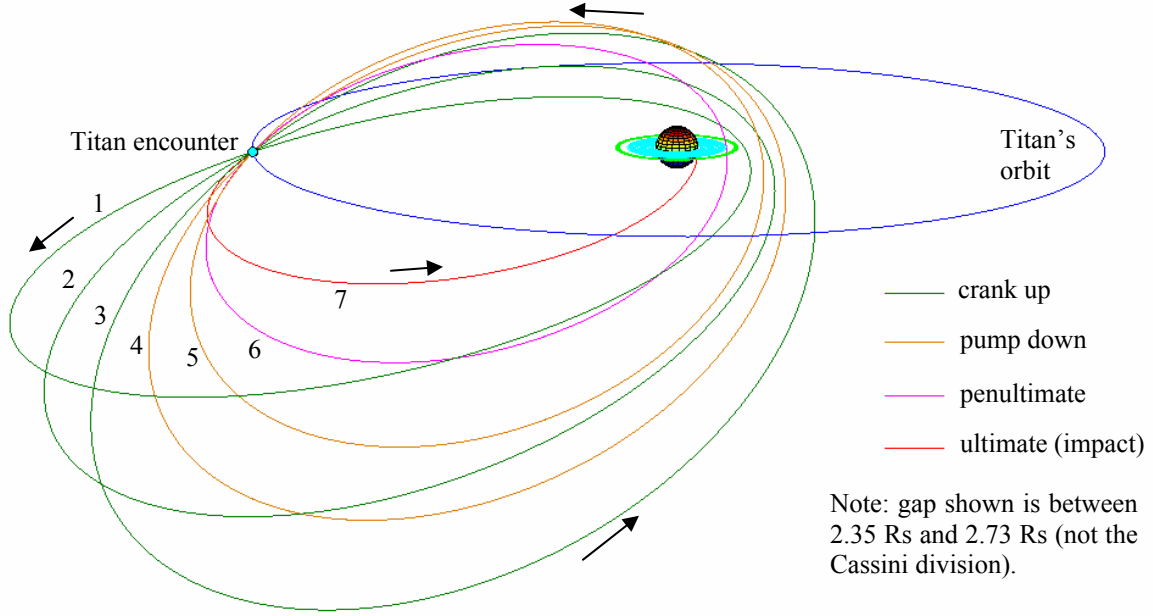

Figure 8: Saturn impact trajectory via ring gap hopping.

Table 6: Short-Period Saturn Impact Trajectory

Event	Titan: S/C	Encounter Date[yyyy/ mm/dd]	In/ Out	h_p [km]	θ [deg]	v_∞ [km/s]	Period [day][a]	r_p [R$_S$][b]	Inc. [deg][c]	r_{vac} [R$_S$][d]	TOF [days][e]
1	1:1	2010/06/21	Out	1000	-93	5.49	15.9	2.96	18.4	3.17	15.9
2	1:1	2010/07/07	Out	1000	-98	5.49	15.9	3.82	32.0	4.17	15.9
3	1:1	2010/07/22	Out	1000	-103	5.49	15.9	5.19	41.8	5.82	15.9
4	3:4	2010/08/07	Out	1000	-164	5.49	12.0	4.50	50.2	4.82	47.8
5	3:5	2010/09/24	Out	1000	-173	5.49	9.57	3.84	58.0	3.98	47.8
6	1:2	2010/11/11	Out	1413	139	5.49	7.97	2.33	62.0	2.36	15.9
7	N/A	2010/11/27	Out	1000	104	5.49	7.13	0.99	60.0	1.00	5.0[f]

[a] Post-flyby orbital period.
[b] Post-flyby periapsis radius.
[c] Post-flyby inclination relative to Saturn's equator.
[d] Post-flyby vacant node crossing distance.
[e] Time of flight to the next Titan encounter.
[f] Impact occurs 5.0 days after the final Titan flyby.

Option 2: Saturn Impact via Long-Period Orbit

We investigate the effect of solar gravity for orbits in quadrants I and III to lower periapsis. With a sufficiently large orbit, the spacecraft can impact Saturn with low ΔV or without a maneuver at apoapsis.

Titan Flyby

Our analysis for a long-period impact originates with initial conditions from STOUR for an outbound Titan flyby on June 15, 2009 (after a series of pumping up the period from *ICA* in Table 2). We assume that the pre-flyby orbit is in a 7:1 resonance with Titan, which is associated with a period of 112 days. It is inclined at 0° with respect to Saturn's equator, corresponding to a 26.7° inclination with respect to Saturn's ecliptic plane. The periapse radius prior to the Titan flyby is 3.91×10^5 km, or 6.49 R_S.

The flyby conditions (i.e., flyby altitude and B-plane angle) are adjusted to yield post-flyby orbits of different periods. The inclination of these particular post-flyby trajectories relative to Saturn's ecliptic plane is 20.7°. The selected orbits lie in quadrant III at an approximate quadrant angle of $\phi_{III} = 39°$. If solar gravity is not modeled, the periapse radii of the post-flyby orbits will range from 5.26×10^5 km (8.72 R_S) to 5.4×10^5 km (8.96 R_S). However, solar gravity significantly affects the orbits, resulting in naturally reduced periapse radii.

Results

We examine two large post-flyby orbits with periods of 877 days and 957 days. After departing the region of Titan, the trajectories reach apoapse radii of 3.51×10^7 km (582.4 R_S) and 3.73×10^7 km (i.e., 619.5 R_S), respectively. Although no ΔV is applied, solar gravity slows the spacecraft and decreases the periapse radius of each orbit. The subsequent periapse radius of the 877-day orbit is therefore 6.89×10^4 km (1.14 R_S), and the periapse radius of the 957-day orbit is 2.58×10^4 km (0.43 R_S).

While the 957-day orbit impacts Saturn without crossing the ring plane, the 877-day orbit crosses the ring plane before periapsis (as illustrated in Figure 9). A ΔV may be implemented at apoapsis to further lower the periapsis if desired. With a ΔV of 10 m/s applied at apoapsis, the periapse radius of the 877-day orbit becomes 4.98×10^4 km (0.83 R_S), and the spacecraft impacts Saturn without crossing the ring plane.

We also investigate two smaller orbits. For a post-flyby orbit with a period of 478 days, the periapse radius is 6.19 R_S if no ΔV is applied. With a maneuver of 135 m/s at apoapsis, the periapse radius is reduced to 1.03 R_S.

For an orbit with a period of 558 days, the periapse radius is 5.28 R_S when no ΔV is applied. With a ΔV of 105 m/s applied at apoapsis, the periapse radius is reduced to 1.06 R_S. These results are summarized in Table 7. Note that the orientation angle is not affected by any maneuver.
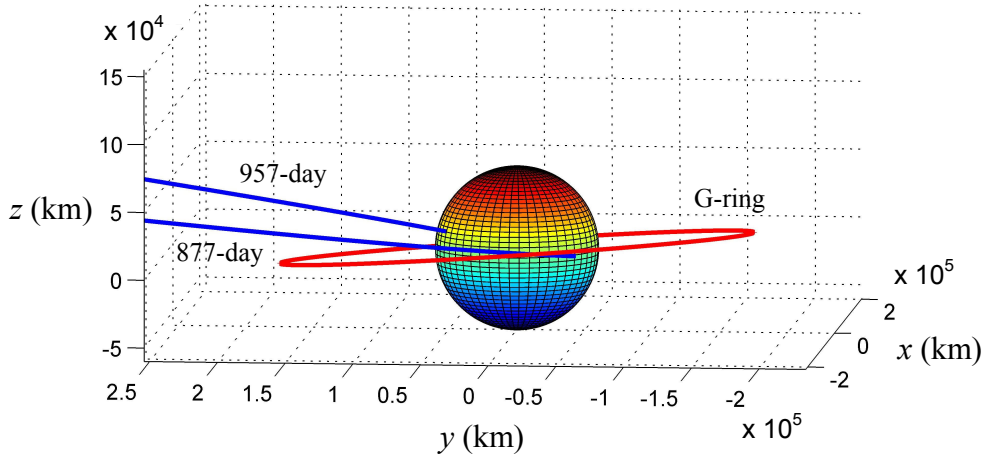
Figure 9: Saturn impact from large orbits with 957-day and 877-day periods (no apoapsis ΔV applied; Earth equator and equinox of J2000 frame).

Table 7: ΔV at Apoapsis and Subsequent Periapse Radii

Period	ΔV, m/s	Post-maneuver r_p, R_S	ϕ_{III} at Apoapsis
478 days	0	6.1981	46.0°
478 days	135	1.0341	46.0°
558 days	0	5.2826	45.1°
558 days	105	1.0610	45.1°
877 days	0	1.1439	40.3°
877 days	10	0.8258	40.3°
957 days	0	0.4293	39.0°

Given the flyby conditions corresponding to this tour and this final Titan encounter, the fate of the spacecraft may be summarized as follows. When the spacecraft is in an orbit with a Keplerian period of approximately 900 days or greater, with apoapsis appropriately oriented in quadrant I or III, it can impact Saturn without an applied ΔV at apoapsis. For an orbit with a period smaller than 900 days, the effects of solar gravity may not be sufficiently large to drop periapsis below 1 R_S, in which case a ΔV must be applied at apoapsis to compensate. With an applied ΔV at apoapsis of about 100 m/s, a spacecraft in an orbit with a Keplerian period of about 550 days can impact Saturn.

While the specifics will change with different post-flyby conditions, these particular examples may serve as a guide in relating orbit size and apoapse ΔV requirements for Saturn impact. Titan encounters can be used to deliver the spacecraft to orbits of different periods and orientations as desired. Minor adjustments to orientation and inclination (via the final Titan encounter) can change the impact conditions.

Orientation and Inclination Requirements
    The orbital period requirement of 900 days is approximate and will depend on the inclination and orientation of the orbit as well as the epoch and initial periapse radius of the orbit. For a

900-day orbit, orientation of the trajectory must be within ±10º of the optimal orientation to achieve impact without an applied ΔV. The optimal orientation is approximately 45º, though it varies depending on the quadrant and the size of the orbit. For larger orbits, this "window" of acceptable orientations expands. The optimal inclination of the orbit is 0º relative to the ecliptic plane. For 900-day orbits, impact has been confirmed for inclinations up to 40º relative to the ecliptic plane; larger inclinations may be acceptable.

Since no optimization process has been employed in our analysis to determine an optimal orbit inclination or orientation, it may be possible to lower the required initial Keplerian period or the required ΔV at apoapsis reported here.

V.   Conclusions

Several end-of-life scenarios are being considered for the Cassini mission, including injection into a 500-year stable orbit within the Saturnian system, escape from Saturn to impact on Jupiter, Uranus, or Neptune, and impact in the Saturnian atmosphere itself. In this paper, we present two methods of causing the spacecraft to impact Saturn's atmosphere: one involving a short-period orbit and one involving a long period orbit. In the short-period case, care must be taken (via a new application of the Tisserand graph) to deftly avoid collision with the rings during multiple ring plane crossings while guaranteeing atmospheric entry. In the long-period case, the spacecraft orbit is pumped up so that a small maneuver at apoapsis ensures atmospheric entry. In particular, if the final orbit has a period greater than 900 days and has the correct orientation, then solar perturbations automatically lowers the periapsis into the atmosphere, so that the final Titan flyby, if performed accurately enough, provides a "flyby-and-forget" option.

Acknowledgements

Notation

Symbols

a = semi-major axis, km or R_S
e = eccentricity
h = specific angular momentum, km^2/s
h_p = flyby altitude, km
i_{rel} = inclination relative to the gravity-assist body's orbit, deg
m = number of spacecraft orbits about the central body
n = number of gravity-assist body orbits about the central body
p = semi-latus rectum, km or R_S
$\boldsymbol{r}$ = position vector from the central body, km or R_S
r = radial distance from center of Saturn to spacecraft, km or R_S
r_a = radius of apoapsis from central body, km or R_S
r_{enc} = radial distance of encounter from central body, km or R_S
r_p = radius of periapsis from central body, km or R_S
r_{vac} = radial distance of vacant node from central body, km or R_S
R_S = Saturn's radius, km (1 R_S = 60268 km)
R_T = Titan's radius, km (1 R_T = 2575 km)
T = orbital period, day
$\mathbf{V}$ = velocity vector relative to the central body, km/s
v = velocity magnitude relative to the central body, km/s
$\mathbf{V_\infty}$ = hyperbolic excess velocity vector, km/s
v_∞ = hyperbolic excess velocity magnitude, km/s
α = pump angle, deg
ΔV = change in velocity magnitude, km/s
δ = flyby bending angle, deg
ϕ = orientation of the spacecraft orbit relative to the Sun-Saturn line, deg
γ = flight path angle, deg
κ = crank angle, deg
μ = gravitational parameter (GM), km^3/s^2
θ = flyby B-plane angle, deg

Subscripts

cb = quantity for central body
ga = quantity for the gravity-assist body
in = quantity for incoming flyby
out = quantity for outgoing flyby
sc = quantity for the spacecraft
I   = quantity for quadrant I
II   = quantity for quadrant II
III   = quantity for quadrant III
IV   = quantity for quadrant IV

References

[1] Mitchell, R. T., "Cassini/Huygens at Saturn and Titan," IAC-05-A3.2.A.01, 56th International Astronautical Congress, Fukuoka, Japan, Oct. 17-21, 2005.

[2] Spencer, J., The Planetary Society Weblog, "Cassini's Extended Mission Tour," Feb. 5, 2007, *http://www.planetary.org/blog/article/00000850*.

[3] Bindschadler, D. L., Theilig, E. E., Schimmels, K. A., and Vandermey, N., "Project Galileo: Final Mission Status," IAC-03-Q.2.01, 54th International Astronautical Congress, Bremen, Germany, Sep. 29–Oct. 3, 2003.

[4] Strange, N. J., Goodson, T. D., and Hahn, Y., "Cassini Tour Redesign for the Huygens Mission," AIAA 2002-4720, AIAA/AAS Astrodynamics Specialist Conference, Monterey, California, Aug. 5-8, 2002.

[5] Smith, J. C., "Description of Three Candidate Cassini Satellite Tours," AAS 98-106, AAS/AIAA Space Flight Mechanics Meeting, Monterey, California, Feb. 9-11, 1998.

[6] Wolf, A. A., "Touring the Saturnian System," *Space Science Reviews*, Vol. 104, 2002, pp. l01-128.

[7] Wolf, A. A., and Smith, J. C., "Design of the Cassini Tour Trajectory in the Saturnian System", *Control Engineering Practice*, Vol. 3, No. 11, Oct. 1995, pp. 1611-1619.

[8] Uphoff, C., Roberts, P. H., and Friedman, L. D., "Orbit Design Concepts for Jupiter Orbiter Missions," *Journal of Spacecraft and Rockets*, Vol. 13, No. 6, June 1976, pp. 348-355.

[9] Vandermey, N., and Paczkowski, B. G., "The Cassini-Huygens Mission Overview," AIAA 2006-5502, AIAA 9th International Conference on Space Operations (SpaceOps), Rome, Italy, June 19-24, 2006.

[10] Patterson, C., Kakoi, M., Howell, K. C., Yam, C. H., and Longuski, J. M., "500-Year Eccentric Orbits for the Cassini Spacecraft within the Saturn System," AAS 07-256, AAS/AIAA Astrodynamics Specialist Conference, Mackinac Island, Michigan, Aug. 19-23, 2007.

[11] Davis, D. C., Patterson, C., and Howell, K. C., "Solar Gravity Perturbations to Facilitate Long-Term Orbits: Application to Cassini," AAS 07-275, AAS/AIAA Astrodynamics Specialist Conference, Mackinac Island, Michigan, Aug. 19-23, 2007.

[12] Okutsu, M., Yam, C. H., Longuski, J. M., and Strange, N. J., "Cassini End-of-Life Escape Trajectories to the Outer Planets," AAS 07-258, AAS/AIAA Astrodynamics Specialist Conference, Mackinac Island, Michigan, Aug. 19-23, 2007.

[13] European Space Agency, "Cassini Saturn Orbiter and Titan Probe, ESA/NASA Assessment Study," ESA REF: SCI(85)1, Aug. 1985.

[14] Spilker, L. J. (Editor), *Passage to a Ringed World*, NASA SP-533, Oct. 1997, NASA Special Publication, *http://saturn.jpl.nasa.gov/multimedia/products/product-references.cfm*.

[15] Miner, E. D., "The Cassini-Huygens Mission to Saturn and Titan," Astronomical Data Analysis Software and Systems XI, *ASP Conference Proceedings*, Vol. 281, 2002, pp. 373-381.

[16] Matson, D. L., Spilker, L. J., and Lebreton, J.-P., "The Cassini/Huygens Mission to the Saturnian System," *Space Science Reviews*, Vol. 104, No. 1-4 , July, 2002, pp. 1-58.

[17] Cuzzi, J. N., Colwell, J. E., Esposito, L. W., Porco, C. C., Murray, C.D., Nicholson, P.D., Spilker, L. J., Marouf, E. A., French, R. C., Rappaport N., and Muhleman, D., "Saturn's Rings: Pre-Cassini Status and Mission Goals," *Space Science Reviews*, Vol. 104, No. 1-4, July, 2002, pp. 209-251.

[18] Porco, C. C., Helfenstein, P., Thomas, P. C., Ingersoll, A. P., Wisdom, J., West, R., Neukum, G., Denk, T., Wagner, R., Roatsch, T., Kieffer, S., Turtle, E., McEwen, A., Johnson, T. V., Rathbun, J., Veverka, J., Wilson, D., Perry, J., Spitale, J., Brahic, A., Burns, J. A., DelGenio, A. D., Dones, L., Murray, C. D., and Squyres, S., "Cassini Observes the Active South Pole of Enceladus," *Science*, Mar. 10, 2006, Vol. 311, No. 5766, pp. 1393-1401.

[19] Hansen, C. J., Esposito, L., Stewart, A. I. F., Colwell, J., Hendrix, A., Pryor, W., Shemansky, D., and West, R., "Enceladus' Water Vapor Plume," *Science*, Mar. 10, 2006, Vol. 311, No. 5766, pp. 1422-1425.

[20] Stofan, E. R., Elachi, C., Lunine, J. I., Lorenz, R. D., Stiles, B., Mitchell, K. L., Ostro, S., Soderblom, L., Wood, C., Zebker, H., Wall, S., Janssen, M., Kirk, R., Lopes, R., Paganelli, F., Radebaugh, J., Wye, L., Anderson, Y., Allison, M., Boehmer, R., Callahan, P., Encrenaz, P., Flamini, E., Francescetti, G., Gim, Y., Hamilton, G., Hensley, S., Johnson, W. T. K., Kelleher, K., Muhleman, D., Paillou, P., Picardi, G., Posa, F., Roth, L., Seu, R., Shaffer, S., Vetrella, S., and West, R., "The lakes of Titan," *Nature*, Vol. 445, No. 7123, Jan. 4, 2007, pp. 61-64.

[21] Spitale, J. N., Jacobson, R. A., Porco, C. C., and Owen, W. M. Jr., "The Orbits of Saturn's Small Satellites Derived from Combined Historic and Cassini Imaging Observations," *The Astronomical Journal*, Vol. 132, No. 2, Aug. 2006, pp. 692-710.

[22] Porco, C. C., Baker, E., Barbara, J., Beurle, K., Brahic, A., Burns, J. A., Charnoz, S., Cooper, N., Dawson, D. D., Del Genio, A. D., Denk, T., Dones, L., Dyudina, U., Evans, M. W., Giese, B., Grazier, K.,

Helfenstein, P., Ingersoll, A. P., Jacobson, R. A., Johnson, T. V., McEwen, A., Murray, C. D., Neukum, G., Owen, W. M., Perry, J., Roatsch, T., Spitale, J., Squyres, S., Thomas, P., Tiscareno, M., Turtle, E., Vasavada, A. R., Veverka, J., Wagner, R., and West, R., "Cassini Imaging Science: Initial Results on Saturn's Rings and Small Satellites," *Science*, Vol. 307, No. 5713, Feb. 25, 2005, pp. 1226-1236.

[23] Flanagan, S. and F. Peralta, "Cassini 1997 VVEJGA Trajectory Launch/Arrival Space Analysis," AAS Paper 93-684, AAS/AIAA Astrodynamics Conference, Victoria, Canada, Aug. 1993.

[24] Lebreton, J-P., Witasse, O., Sollazzo, C., Blancquaert, T., Couzin, P., Schipper, A-M., Jones, J. B., Matson, D. L., Gurvits, L. I., Atkinson, D. H., Kazeminejad, B., and Pérez-Ayúcar, M., "An Overview of the Descent and Landing of the Huygens probe on Titan," *Nature*, Vol. 438, No. 7069, Dec. 8, 2005, pp. 758-764.

[25] Sollazzo, C., Wheadon, J., Lebreton, J-P., Clausen, K., Blancquaert, T., Witasse, O., Pérez-Ayúcar, M., Schipper, A.-M., Couzin, P., Salt, D., Hermes, M., and Johnsson, M., "The Huygens Probe Mission to Titan: Engineering the Operational Success," AIAA-2006-5503, SpaceOps 2006 Conference, Rome, Italy, June 19-23, 2006.

[26] Goodson, T. D., Buffington, B. B., Hahn, Y., Strange, N. J., Wagner, S. V., and Wong, M. C., "Cassini-Huygens Maneuver Experience: Cruise and Arrival at Saturn," AAS 05–286, AAS/AIAA Astrodynamics Specialist Conference, Lake Tahoe, California, Aug. 7-11, 2005.

[27] Standley, S. P., "Cassini-Huygens Engineering Operations at Saturn," AIAA-2006-5516, SpaceOps 2006 Conference, Rome, Italy, June 19-23, 2006.

[28] Wagner, S., Gist, E. M., Goodson, T. D., Hahn, Y., Stumpf, P. W., and Williams, P. N., "Cassini-Huygens Maneuver Experience: Second Year of Saturn Tour," AIAA 2006-6663, AIAA/AAS Astrodynamics Specialist Conference and Exhibit, Keystone, Colorado, Aug. 21-24, 2006.

[29] The Planetary Society Space Topics: Cassini-Huygens, "Cassini's Tour of the Saturn System," Feb. 7, 2007, *http://planetary.org/explore/topics/space_missions/cassini_huygens/tour.html*.

[30] Broucke, R. A., "The Celestial Mechanics of Gravity Assist," AIAA 1988-4220, AIAA/AAS Astrodynamics Conference, Minneapolis, Minnesota, Aug 15-17, 1988.

[31] Cesarone, R. J., "A Gravity Assist Primer," *AIAA Student Journal*, Vol. 27, Spring 1989, pp. 16-22.

[32] Beckman, J. C., and Smith, D. B., "The Jupiter Orbiter Satellite Tour Mission," AAS 73-231, AAS/AIAA Astrodynamics Conf., Vail, Colorado, July 1973.

[33] Strange, N. J., and Sims, J. A., "Methods for the Design of V-Infinity Leveraging Maneuvers," AAS 01-437, AAS/AIAA Astrodynamics Conference, Quebec city, Quebec, Canada, July/Aug. 2001.

[34] Strange, N. J., "Control of Node Crossings in Saturnian Gravity-Assist Tours," AAS 03-545, AAS/AIAA Astrodynamics Specialist Conference, Big Sky, Montana, Aug. 3-7, 2003.

[35] Roy, A. E., *Orbital Motion*, 2nd ed., Adam Hilger, Bristol, England, United Kingdom, 1982, pp. 129,130.

[36] Labunsky, A. V., Papkov, O. V., and Sukhanov, K. G., *Multiple Gravity Assist Interplanetary Trajectories*, 1st ed., Gordon and Breach Science Publishers, Amsterdam, 1998, pp. 101-197.

[37] Strange, N. J., and Longuski, J. M., "Graphical Method for Gravity-Assist Tour Design," *Journal of Spacecraft and Rockets*, Vol. 39, No. 1, 2002, pp. 9-16.

[38] Heaton, A. F., Strange, N. J., Longuski, J. M., and Bonfiglio, E. P., "Automated Design of the Europa Orbiter Tour," *Journal of Spacecraft and Rockets*, Vol. 39, No. 1, 2002, pp. 17-22.

[39] Strange, N. J., "Pumping, Cranking and Bending," JPL Internal Presentation, Mar. 30-Apr. 3, 2006.

[40] Rinderle, E. A., "Galileo User's Guide, Mission Design System, Satellite Tour Analysis and Design Subsystem," Jet Propulsion Laboratory, JPL Internal Document D-263, California Institute of Technology, Pasadena, California, July 1986.

[41] Yamakawa, H., Kawaguchi, J., Ishil, N., and Matsuo, H., "On Earth-Moon Transfer Trajectory with Gravitational Capture," AAS paper 93-633, AAS/AIAA Astrodynamics Specialist Conference, Victoria, Canada, Aug. 16-19, 1993.

[42] Williams, S. N., "Automated Design of Multiple Encounter Gravity-Assist Trajectories," M.S. Thesis, School of Aeronautics and Astronautics, Purdue University, West Lafayette, Indiana, Aug. 1990.

[43] Longuski, J. M., and Williams, S. N., "Automated Design of Gravity-Assist Trajectories to Mars and the Outer Planets," *Celestial Mechanics and Dynamical Astronomy*, Vol. 52, No. 3, 1991, pp. 207–220.

[44] Patel, M. R., "Automated Design of Delta-V Gravity-Assist Trajectories for Solar System Exploration," M. S. Thesis, School of Aeronautics and Astronautics, Purdue University, West Lafayette, Indiana, Aug. 1993.

[45] Bonfiglio, E. P., "Automated Design of Gravity-Assist and Aerogravity-Assist Trajectories" M. S. Thesis, School of Aeronautics and Astronautics, Purdue University, West Lafayette, Indiana, Aug. 1999.

[46] Howell, K. C., and Anderson, J., *User's Guide: Purdue Software GENERATOR*, School of Aeronautics and Astronautics, Purdue University, West Lafayette, Indiana, July 2001.